PHYSICAL REVIEW A **77**, 051403(R) (2008)

Radial compression of a non-neutral plasma in a cusp trap for antihydrogen synthesis

H. Saitoh,[1,*] A. Mohri,[1] Y. Enomoto,[1,2] Y. Kanai,[1] and Y. Yamazaki[1,2]
[1]*Atomic Physics Laboratory, RIKEN, 2-1 Hirosawa, Wako, Saitama 351-0198, Japan*
[2]*Institute of Physics, The University of Tokyo, 3-8-1 Komaba, Meguro, Tokyo 153-8902, Japan*
(Received 29 October 2007; published 27 May 2008)

We present the radial compression of an electron plasma by using a rotating wall in a spindle cusp region of an axisymmetric magnetic quadrupole. The compression rate depended on the rotating frequencies and had a broad peak extending on both sides of a longitudinal (1,0) mode frequency, which was the only observed characteristic frequency. The formation of the high-density plasma is one of the important milestones for the antihydrogen formation and extraction of ultraslow spin-polarized antihydrogen beams in the spindle cusp.

DOI: 10.1103/PhysRevA.77.051403 PACS number(s): 37.10.−x, 52.27.Jt, 36.10.−k, 52.27.Aj

Spectroscopic comparison of antihydrogen atoms with hydrogen ones is one of the best candidates for the stringent tests of the CPT symmetry. Studies in handling cold antiprotons are being carried out intensively by using the antiproton decelerator (AD) facility [1] at CERN and two groups have succeeded the production of cold antihydrogen atoms [2,3]. In the experiments carried out so far, 5.3 MeV antiprotons from the AD were decelerated, trapped, and mixed with positrons to form antihydrogen atoms via recombination processes in uniform magnetic fields of "nested" Penning traps.

For efficient production of antihydrogen atoms, a technique to form high-density antiproton and positron plasmas is one of the essential issues. A rotating wall, i.e., application of a rotating electric field to non-neutral plasmas, proved to be a useful method to manipulate charged particles in a homogeneous magnetic field [4–10]. The rotating wall was applied to control confinement properties and rotation speed of ion plasmas [4,5,7], and it was also used for transport control of electron [6–9] and positron [10] plasmas. The compression at resonant frequencies around the Trivelpiece-Gould modes was examined by several groups [6–8]. A so-called "strong drive" used a large amplitude of a rotating wall field [9,10], where the compression became possible at a broad range of frequencies and the central density of the plasma increased until the plasma rotation frequency equaled the applied rotating wall frequency.

For future experiments on high-precision laser or microwave spectroscopy of antihydrogen, it is required that the generated antihydrogen atoms in high Rydberg states are trapped for a time long enough to cascade down to their ground state [11–13]. Antihydrogen atoms with magnetic moment μ undergo $-\mu\nabla|\mathbf{B}|$ force in an inhomogeneous magnetic field $\mathbf{B}$, and thus cold antihydrogen atoms in the low-field seeking states can in principle be confined in minimum-B magnetic field configurations [14,15]. However, it is not straightforward to superpose a magnetic gradient on Penning-Malmberg traps and to simultaneously confine both neutral atoms and non-neutral plasmas. In the standard Ioffe-Pritchard trap [16], the quadrupole field of Ioffe bars breaks the axial symmetry of a magnetic configuration, which may lead to instability or rapid losses of non-neutral plasmas [17]. A new experiment was proposed for antihydrogen spectroscopy by using a trap with octupole magnetic field for reducing the field asymmetry and resultant perturbations. Non-neutral plasmas of antiprotons and positrons were sustained without significant diffusive loss [18].

The use of an axisymmetric magnetic quadrupole for non-neutral plasma confinement, i.e., cusp trap, provides another potential scheme to synthesize and trap cold antihydrogen atoms in the ground state [12,19–22]. This field is provided by a set of anti-Helmholtz coils. When antiproton and positron clouds are mixed near the magnetic null point of the cusp trap, cold antihydrogen atoms are synthesized and extracted as ultraslow spin-polarized beams. Numerical study has shown the existence of a rigid-rotor equilibrium of cold non-neutral plasma in the nonuniform magnetic field of a spindle cusp [21]. In this study, we have experimentally investigated the properties of the electron plasma in a spindle cusp, such as the stability, the oscillation modes, the cooling feature, and particularly the radial transport. We applied a rotating wall technique to the plasma and found a way to make an effective radial compression. Although the application of the rf field of the rotating wall heated up the plasma, the synchrotron radiation in the strong cusp magnetic field quickly cooled the plasma, and as a result a cold and high-density plasma was successfully formed.

Figure 1 shows the schematic view of the trap and field profiles in the superconducting cusp magnet [21]. The trap system was evacuated to a base pressure of 2×10^{-7} Pa. Electrons were trapped by the combination of a cusp magnetic field and an electrostatic potential. The cusp field is expressed by a vector potential $A_\theta(r,z)=(B_0/L)rz$ in the cylindrical coordinates (r,θ,z). The maximum field strength on the center axis of the device is 2.0 T at $z=\pm150$ mm when the coil current is 60 A. In the confinement region of the trap, the typical field strength in this experiment is 1.6 T at $z=\pm80$ mm. The variation of the field strength at $z=40-120$ mm is 55%. The trap consists of 12 cylindrical electrodes with an inner diameter of 80 mm and lengths of 14 mm (G1,G2,F1,F2), 30 mm (G3–F5,F3–F5), and 73 mm (G6,F6), crespectively. In the trap region, a harmonic electrostatic potential $\phi_V(r,z)=-\phi_0[(z-L)^2-r^2]/L^2$ was applied. As shown in Fig. 1(c), the potential well for an electron trap was centered at the position of $z=L=+80$ mm. Here ϕ_0/L^2 was set in a range from 3.6×10^3 to 1.1×10^4 V/m^2 in the

*Present address: Department of Advanced Energy, The University of Tokyo, 5-1-5 Kashiwanoha, Chiba 277-8561, Japan.

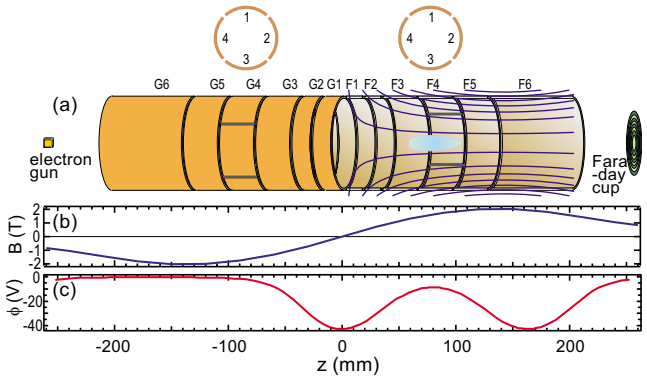

FIG. 1. (Color online) (a) Schematic view of the trap electrodes, field lines, and confined plasma. Electrodes G4 and F4 produce rotating wall rf fields. (b) Magnetic field strength profile at the coil current of 60 A, (c) electrostatic potential profile in the confinement phase on the device axis $r=0$.

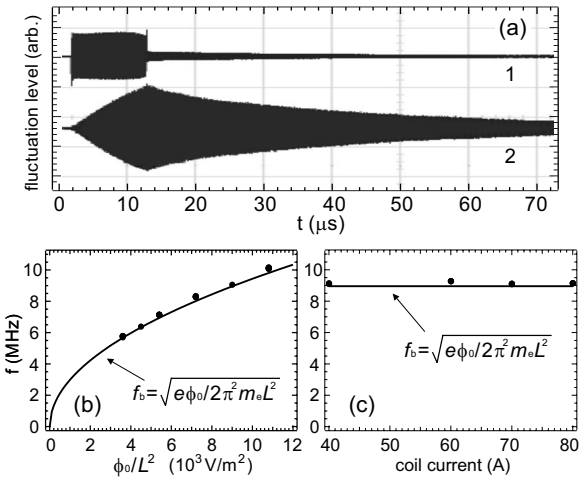

FIG. 2. (a) Response of plasma on the external longitudinal rf electric field at the resonance frequency. Ch1: External rf voltage of $f=8.9$ MHz and $V=0.4$ V added on electrode F5, and ch2: excited fluctuation received on electrode F3. Resonant frequencies f_z as functions of (b) gradient of the external electrostatic potential well, represented by ϕ_0/L^2, and (c) cusp magnetic field strength.

experiment. In the most often used case, $\phi_0/L^2=9.0\times10^3$ V/m^2 and the depth of the potential well was 30 V. The longitudinal bounce motion of an electron in the potential well is approximated as a harmonic oscillation with a frequency of $f_b=\sqrt{e\phi_0/2\pi^2 m_e L^2}=9.0$ MHz. An azimuthally rotating $m=1$ electric field was applied to the plasma by using the fourfold segmented electrode F4. Sinusoidal rf on the electrode segments had phase differences of $\pi/2$ in the direction parallel or opposite to the $\mathbf{E}\times\mathbf{B}$ plasma rotation and f_{RW} was<15 MHz.

Electrons were injected by an electron gun with an iridium-coated barium-impregnated cathode as a train of pulsed beams. The typical number of the pulses, the duration of each pulse, and the duty cycle were 30, 10 μs, and 10%, respectively. During the injection phase, the potential wall on the electron gun side was lowered synchronously to the arrival of each beam pulse and thereby electrons were trapped inside the potential well. The initially trapped electron number N_0 was $10^7<N_0<10^9$. The reproducibility of N_0 was quite good and the fluctuation $\delta N_0/N_0<2\%$. After the injection period, the rotating wall was applied. Then electrons were dumped on a Faraday cup located at the downstream side of the trap [see Fig. 1(a)]. The Faraday cup is coaxially segmented into eight with the radial pitch of 4 mm and the total diameter is 60 mm, which allows us to monitor the line-integrated density n_l (integration of density along magnetic field lines) of the electron plasma. The dumped charge on each segment in the series of injection-trap-dump cycle gives the temporal evolution of n_l. We also studied the parallel temperature of an electron plasma by shallowing the potential wall and analyzing the energy profiles of escaping electrons [23].

By applying a white noise or sweeping the frequency of a sinusoidal wave on electrode F5, we searched for excited oscillation modes from 10 kHz to 30 MHz by monitoring the induced signals on electrode F3. Here, one resonant mode corresponding to the center-of-mass oscillation of an electron plasma was detected. As shown in Fig. 2(a), when the external rf of this mode frequency was applied, the oscillation amplitude grew almost linearly. When the external rf was turned off, the amplitude decayed exponentially with a time constant of 35 μs. Figures 2(b) and 2(c) show the frequencies of the observed oscillation mode f_z as functions of ϕ_0 and the magnetic field strength B. The mode frequency had a dependence of $f_z\propto E^{1/2}B^0$, where E is the external electric field strength. Actually, the solid curve f_b in Fig. 2(b) reproduces the observed mode frequencies quite satisfactorily. These observations suggest that the detected mode resembles the center-of-mass oscillation of an electron plasma in a harmonic potential well. In fact, although the electron temperature varied during the confinement cycle, as discussed later, the observed frequency stayed constant [24]. No other resonance frequency was found for 10 kHz$<f<$15 MHz, possibly due to the effects of inhomogeneous magnetic field of the spindle cusp.

Figures 3(a) and 3(b) show temporal evolution of n_l profiles with and without the application of a rotating wall. The initial electron number and plasma radius were $N_0=5.7\times10^7$ and approximately 5 mm, respectively. According to an equilibrium analysis of non-neutral plasmas in the spindle cusp [21], the electron number density and azimuthal rotation frequency were calculated as $n_e=6\times10^7$ cm^{-3} and $f_{rot}=60$ kHz for the above plasma parameters and applied electromagnetic configuration. The observed frequency of the longitudinal oscillation was $f_z=8.9$ MHz. When the rotating wall was not applied, the plasma radially expanded as shown in Fig. 3(a). In this case, the total electron number decreased after $t\sim400$ s. As is shown by the solid circles and the dotted line in Fig. 3(c), the line-integrated density at $r=0$ was $n_{l(r=0)}=6.7\times10^4$ cm^{-2} at $t=1$ s, and decreased to $n_{l(r=0)}=7.2\times10^3$ cm^{-2} at $t=1000$ s with a time constant of $\tau_E=150$ s. The total charge decreased with a $1/e$ time constant of 3000 s.

In contrast, by applying the rotating wall in an appropriate frequency range, effective compression of the plasma was observed as is shown in Fig. 3(b). The rotating wall was applied in the direction of the $\mathbf{E}\times\mathbf{B}$ rotation of the plasma at

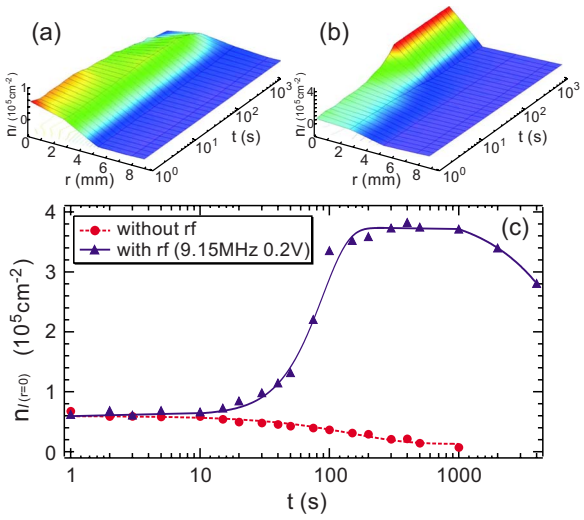

FIG. 3. (Color online) Temporal evolution of the line-integrated density profiles of a plasma (a) with and (b) without the rotating wall, and (c) n_l: line-integrated density at $r=0$. The solid and dotted lines are to guide the eyes only.

the frequency of $f_{RW}=9.15$ MHz, which was 0.25 MHz higher than f_z. The amplitude of the applied rf was $V_{RW}=0.2$ V. The solid triangles and the solid line in Fig. 3(c) show that n_l increased in a time scale of the order of 10^2 s, and it saturated at $t\sim400$ s, where $n_{l(r=0)}=3.8\times10^5$ cm^{-2} with an enhancement by a factor of 6 from $t=0$. After the application of the rotating wall for 400 s, 74% of the initial electrons were radially compressed into the central region ($r<1.4$ mm). Both the total charge and $n_{l(r=0)}$ decreased for $t>1000$ s after the realization of the peaked density profiles. The decay time constant of the plasma charge from $t=500$ to 4000 s, estimated from the total charge dumped on the Faraday cup electrodes, was 1.3×10^4 s (3.3 h). When the rotating wall was turned off after the radial compression, the plasma gradually expanded with almost the same time constant as that without the rotating wall from the beginning.

Figure 4 shows the central line-integrated density $n_{l(r=0)}$ and the total electron number N_t after the application of the rotating wall for 20 s. When the rotating wall was not applied, $n_{l(r=0)}=2.1\times10^4$ cm^{-2}. When the rotating wall was applied in the $\mathbf{E}\times\mathbf{B}$ rotation direction, radial compression was observed in a broad f_{RW} range from approximately 6 to 9.5 MHz except for frequencies from 8.85 to 9.0 MHz. When f_{RW} was close to the observed longitudinal resonance mode frequency of $f_z=8.9$ MHz, both the numbers of electrons in the central region and the total electrons decreased quickly regardless of the rotation direction ($n_{l(r=0)}=2\times10^2$ cm^{-2} at $t=20$ s).

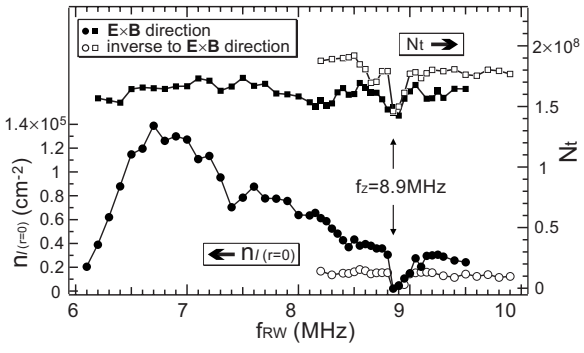

FIG. 4. Total electron number N_t and line-integrated density on the device axis $n_{l(r=0)}$ at $t=20$ s as a function of applied rotating wall frequency. Directions of the applied rotating wall were equal to (solid circles and solid squares) and opposite to (open circles and open squares) the $\mathbf{E}\times\mathbf{B}$ plasma rotation.

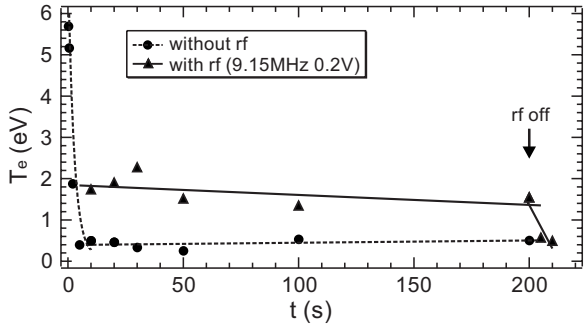

FIG. 5. Temporal evolutions of $T_{e\|}$ when the rotating wall was applied from $t=0$ to 200 s (triangles) and not applied (circles).

Figure 5 shows temporal evolutions of the electron temperature $T_{e\|}$ parallel to $\mathbf{B}$. Just after the electron injection ($t=0.2$ s), $T_{e\|}=5.7$ eV. When the rotating wall field was not applied, it cooled quickly and reached 0.4 eV in $t=10$ s and then stayed constant. Such a steady state is additional evidence of the existence of a rigid-rotor equilibrium of a non-neutral plasma in the spindle cusp configuration. The observed $1/e$ cooling time of $T_{e\|}$ was 2.5 s, which is comparable to the typical cooling time caused by the synchrotron radiation in a magnetic field given by the Larmor formula for the typical field strength $B=1.6$ T: $\tau_D\sim3\pi\varepsilon_0 m_e c^3/e^2\omega_{ec}^2\sim1.0$ s. The parallel electron temperature did not decrease lower than 0.4 eV, which could be due to the effects of the warm bore and external noise. Further study will be carried out in the near future using a cryogenic cusp trap.

The closed triangles in Fig. 5 show the temperature evolution when the rotating wall was turned on, which revealed that it reached an equilibrium of $T_{e\|}=1.7$ eV, four times higher than that without the rotating wall. When the rf was turned off, $T_{e\|}$ dropped to the same temperature 0.4 eV, as in the case of no rf application, and this cooling rate was comparable to τ_D as shown in Fig. 5. The time scale of the radial expansion of the compressed plasma $\tau_E\sim150$ s is much longer than τ_D, and the rotating wall can significantly compress the plasma practically keeping the plasma temperature unchanged.

In future experiments, a positron plasma on one side of a spindle cusp will be transported to the opposite side in order to induce recombinations with antiprotons. In this process, particles located near the center axis of the device are primarily transferred through the magnetic null point, and the plasma may take unstable hollow structures. The rotating wall can be utilized for the stable transfer of positrons by the radial compression that compensate the decrease of particles on the device axis.

To summarize, we have demonstrated that a single-component plasma in the spindle cusp can be effectively compressed by using a rotating wall, as in the case of a plasma in a uniform magnetic field. The compression was observed with a broad frequency range of a rotating wall in the $\mathbf{E}\times\mathbf{B}$ velocity direction except for frequencies close to the longitudinal resonance frequency of the plasma, which is the only observed mode of a spindle cusp electron plasma. The compression and cooling of an electron plasma were realized simultaneously. Although the present experiment was carried out using an electron plasma, the same procedure can in principle be applied to a positron plasma, which is particularly important for the formation and extraction of antihydrogen atoms.

This work was funded by Special Research Projects for Basic Science of RIKEN. The work of H.S. was supported in part by the Special Postdoctoral Researchers Program of RIKEN.

[1] S. Maury, Hyperfine Interact. **109**, 43 (1997).

[2] M. Amoretti, C. Amsler, G. Bonomi, A. Bouchta, P. Bowe, C. Carraro, C. L. Cesar, M. Charlton, M. J. T. Collier, M. Doser, V. Filippini, K. S. Fine, A. Fontana, M. C. Fujiwara, R. Funakoshi, P. Genova, J. S. Hangst, R. S. Hayano, M. H. Holzscheiter, L. V. Jørgensen, V. Lagomarsino, R. Landua, D. Lindelöf, E. Lodi Rizzini, M. Macrì, N. Madsen, G. Manuzio, M. Marchesotti, P. Montagna, H. Pruys, C. Regenfus, P. Riedler, J. Rochet, A. Rotondi, G. Rouleau, G. Testera, A. Variola, T. L. Watson, and D. P. van der Werf, Nature **419**, 456 (2002).

[3] G. Gabrielse, N. S. Bowden, P. Oxley, A. Speck, C. H. Storry, J. N. Tan, M. Wessels, D. Grzonka, W. Oelert, G. Schepers, T. Sefzick, J. Walz, H. Pittner, T. W. Hänsch, and E. A. Hessels Phys. Rev. Lett. **89**, 213401 (2002).

[4] X.-P. Huang, F. Anderegg, E. M. Hollmann, C. F. Driscoll, and T. M. O'Neil, Phys. Rev. Lett. **78**, 875 (1997).

[5] X.-P. Huang, J. J. Bollinger, T. B. Mitchell, and W. M. Itano, Phys. Rev. Lett. **80**, 73 (1998).

[6] F. Anderegg, E. M. Hollmann, and C. F. Driscoll, Phys. Rev. Lett. **81**, 4875 (1998).

[7] E. M. Hollmann, F. Anderegg, and C. F. Driscoll, Phys. Plasmas **7**, 2776 (2000).

[8] Y. Soga, Y. Kiwamoto, and N. Hashizume, Phys. Plasmas **13**, 052105 (2006).

[9] J. R. Danielson and C. M. Surko, Phys. Rev. Lett. **94**, 035001 (2005); Phys. Plasmas **13**, 055706 (2006).

[10] R. G. Greaves and C. M. Surko, Phys. Rev. Lett. **85**, 1883 (2000); Phys. Plasmas **8**, 1879 (2001).

[11] Y. Yamazaki, Phys. Scr., T **T110**, 286 (2004).

[12] T. Pohl, H. R. Sadeghpour, Y. Nagata, and Y. Yamazaki, Phys. Rev. Lett. **97**, 213001 (2006).

[13] W. Bertsche, A. Boston, P. D. Bowe, C. L. Cesar, S. Chapman, M. Charlton, M. Chartier, A. Deutsch, J. Fajans, M. C. Fujiwara, R. Funakoshi, K. Gomberoff, J. S. Hangst, R. S. Hayano, M. J. Jenkins, L. V. Jørgensen, P. Ko, N. Madsen, P. Nolan, R. D. Page, L. G. C. Posada, A. Povilus, E. Sarid, D. M. Silveira, D. P. van der Werf, Y. Yamazaki, Nucl. Instrum. Methods Phys. Res. A **566**, 746 (2006).

[14] T. M. Squires, P. Yesley, and G. Gabrielse, Phys. Rev. Lett. **86**, 5266 (2001).

[15] D. H. Dubin, Phys. Plasmas **8**, 4331 (2001).

[16] D. E. Pritchard, Phys. Rev. Lett. **51**, 1336 (1983).

[17] E. P. Gilson and J. Fajans, Phys. Rev. Lett. **90**, 015001 (2003).

[18] G. Andresen, W. Bertsche, A. Boston, P. D. Bowe, C. L. Cesar, S. Chapman, M. Charlton, M. Chartier, A. Deutsch, J. Fajans, M. C. Fujiwara, R. Funakoshi, D. R. Gill, K. Gomberoff, J. S. Hangst, R. S. Hayano, R. Hydomako, M. J. Jenkins, L. V. Jørgensen, L. Kurchaninov, N. Madsen, P. Nolan, K. Olchanski, A. Olin, A. Povilus, F. Robicheaux, E. Sarid, D. M. Silveira, J. W. Storey, H. H. Telle, R. I. Thompson, D. P. van der Werf, J. S. Wurtele, and Y. Yanazaki, Phys. Rev. Lett. **98**, 023402 (2007).

[19] A. Mohri and Y. Yamazaki, Europhys. Lett. **63**, 207 (2003).

[20] A. Mohri, T. Yuyama, Y. Kiwamoto, Y. Yamazawa, and T. Michishita, Jpn. J. Appl. Phys., Part 2 **37**, L1553 (1998).

[21] A. Mohri, Y. Kanai, Y. Nakai, and Y. Yamazaki, in *Physics with Ultra Slow Antiproton Beams*, AIP Conf. Proc No. 793 (AIP, New York, 2005), p. 147; A. Mohri, H. Saitoh, Y. Kanai, and Y. Yamazaki, in *Procs. 33rd EPS Conf. Plasma Phys.* (EPS, London, 2006), P-4.067.

[22] N. Kuroda, H. A. Torii, K. Yoshiki Franzen, Z. Wang, S. Yoneda, M. Inoue, M. Hori, B. Juhász, D. Horváth, H. Higski, A. Mohri, J. Eades, K. Komaki, and Y. Yamazaki, Phys. Rev. Lett. **94**, 023401 (2005).

[23] B. R. Beck, J. Fajans, and J. H. Malmberg, Phys. Rev. Lett. **68**, 317 (1992).

[24] H. Higaki and A. Mohri, Jpn. J. Appl. Phys., Part 1 **36**, 5300 (1997).